ARL-TR-8625 ● JAN 2019

US Army Research Laboratory

Measurement of the Acoustic-Radar Response of Electronics and Metals by Excitation with a Modal Thruster in a Transverse Electromagnetic Cell

by Gregory J Mazzaro, Kyle A Gallagher, and Kelly D Sherbondy

NOTICES

Disclaimers

The findings in this report are not to be construed as an official Department of the Army position unless so designated by other authorized documents.

Citation of manufacturer's or trade names does not constitute an official endorsement or approval of the use thereof.

Destroy this report when it is no longer needed. Do not return it to the originator.

ARL-TR-8625 ● JAN 2019

US Army Research Laboratory

Measurement of the Acoustic-Radar Response of Electronics and Metals by Excitation with a Modal Thruster in a Transverse Electromagnetic Cell

Gregory J Mazzaro
The Citadel, Charleston, SC

Kyle A Gallagher and Kelly D Sherbondy
Sensors and Electron Devices Directorate, ARL

REPORT DOCUMENTATION PAGE

Form Approved
OMB No. 0704-0188

1. REPORT DATE *(DD-MM-YYYY)*	2. REPORT TYPE	3. DATES COVERED (From - To)
January 2019	Technical Report	1 May–15 August 2018

4. TITLE AND SUBTITLE
Measurement of the Acoustic-Radar Response of Electronics and Metals by Excitation with a Modal Thruster in a Transverse Electromagnetic Cell

5a. CONTRACT NUMBER

5b. GRANT NUMBER

5c. PROGRAM ELEMENT NUMBER

6. AUTHOR(S)
Kyle A Gallagher, Kelly D Sherbondy, and Gregory J Mazzaro

5d. PROJECT NUMBER

5e. TASK NUMBER

5f. WORK UNIT NUMBER

7. PERFORMING ORGANIZATION NAME(S) AND ADDRESS(ES)
US Army Research Laboratory
ATTN: RDRL-SER-U
Aberdeen Proving Ground, MD 21005-5066

8. PERFORMING ORGANIZATION REPORT NUMBER
ARL-TR-8625

9. SPONSORING/MONITORING AGENCY NAME(S) AND ADDRESS(ES)

10. SPONSOR/MONITOR'S ACRONYM(S)

11. SPONSOR/MONITOR'S REPORT NUMBER(S)

12. DISTRIBUTION/AVAILABILITY STATEMENT
Approved for public release; distribution is unlimited.

13. SUPPLEMENTARY NOTES

14. ABSTRACT
A novel technique for exciting radar targets with acoustic and electromagnetic (EM) energy simultaneously is presented. The technique exploits the interaction between the two forms of energy at the target, in a well-controlled acoustic and EM environment, to evaluate the feasibility of standoff acoustic-radar detection of each target. Data recorded on three electronic radar targets and three metallic clutter items, probed by audible acoustic frequencies and UHF radio frequencies, successfully demonstrate acousto-EM interaction.

15. SUBJECT TERMS
radar, acoustic, electromagnetic, interaction, modulation, detection, metallic, electronic, junction

16. SECURITY CLASSIFICATION OF:			17. LIMITATION OF ABSTRACT	18. NUMBER OF PAGES	19a. NAME OF RESPONSIBLE PERSON
a. REPORT	b. ABSTRACT	c. THIS PAGE			Kyle A Gallagher
Unclassified	Unclassified	Unclassified	UU	25	19b. TELEPHONE NUMBER (Include area code) 301-394-0840

Contents

List of Figures

1. Introduction

The US Army Research Laboratory continues to evaluate acoustic radar for the detection and characterization of concealed threats. An initial study of the acoustic-radar effect on metallic cylinders and corner reflectors was performed using a wideband antenna.[1] The study is now extended to handheld electronics and metallic radar-clutter items using a transverse electromagnetic (TEM) cell with the goal of assembling a benchtop apparatus to catalog acoustic-radar responses of targets and clutter across a wide range of acoustic and electromagnetic (EM) frequencies.

An acoustic radar is illustrated in Fig. 1. The transmitter (Tx) consists of an EM wave generator (i.e., an antenna) emitting a single radio frequency f_{RF} and an acoustic-wave generator (i.e., a speaker) emitting a single acoustic frequency f_{audio}. At the target, the EM wave and the acoustic wave interact. One mechanism by which the acoustic and EM waves interact is Doppler shift: the metallic components of the target shake toward and away from the radar, producing positive and negative frequency shifts at multiples of f_{audio} away from f_{RF}.[2,3] Another mechanism is metal–metal contact: the conductive junctions within the target intermittently connect and disconnect, producing amplitude modulation at a rate of f_{audio} onto the carrier frequency f_{RF}.[4,5]

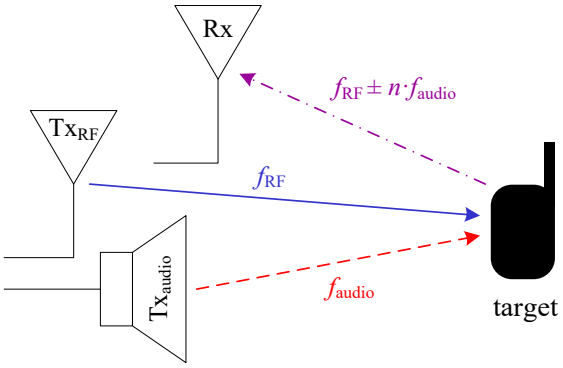

Fig. 1 Acoustic radar for detecting handheld electronics

Because of these interactions and the radar-reflective nature of electronics and metals, the target radiates a new EM wave that consists of the original EM wave modulated by the acoustic wave.[6,7] The new EM wave contains a set of frequencies, $f_{RF} \pm n \cdot f_{audio}$, where n is any positive integer. This acousto-EM response is captured by the radar's receive (Rx) antenna. The presence of measurable EM energy at any discrete multiple of f_{audio} away from the original RF carrier f_{RF} (i.e., at any $n = 0$) indicates target detection.

The authors' previous experiments implemented a horn antenna for EM transmission (Tx_{RF}) and reception. In this work the EM waves are transmitted to/from the target along an open TEM cell. Traditionally used to test electronics for radiated susceptibility, the authors repurposed the TEM cell to study target responses to radar waves.[8] In this study the TEM cell is repurposed again to study target responses to radar waves and acoustic waves that illuminate the target simultaneously.

2. Experiment

The TEM cell is a waveguide structure inside of which each target is placed. The open-wall construction of the cell allows for a modal thruster unit to directly apply an acoustic probe to the target (i.e., to shake it) with a rigid stinger rod, while simultaneously transmitting an EM wave to/from the target along the waveguide. This portion of the experiment is shown in Fig. 2.

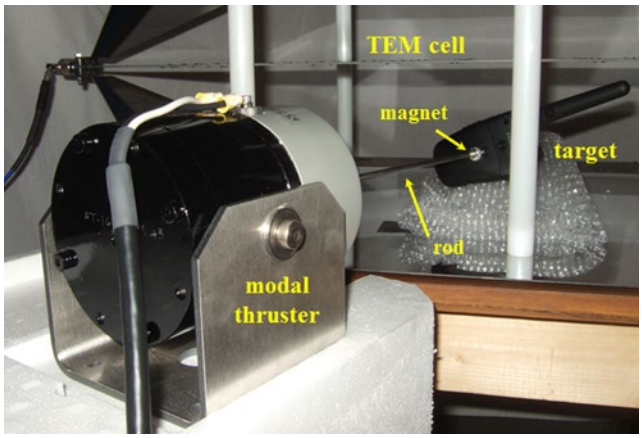

Fig. 2 Modal thruster and TEM cell apparatus used to illuminate targets with acoustic and EM energy simultaneously

A block diagram of the overall experiment used to probe targets with acoustic and EM energy simultaneously is shown in Fig. 3. The EM source is the Agilent N9310A RF signal generator. It outputs a continuous-wave (CW) signal at a frequency f_{RF} and a constant power of $P_{RF} = 0$ dBm. This CW transmit signal enters a MiniCircuits ZGDC6-362HP+ directional coupler and passes on to the TEM cell. The output of the coupler is attached to Port 1 of the Tekbox TBTC3 TEM cell. Port 2 of the TEM cell is terminated in a matched 50-Ω load.

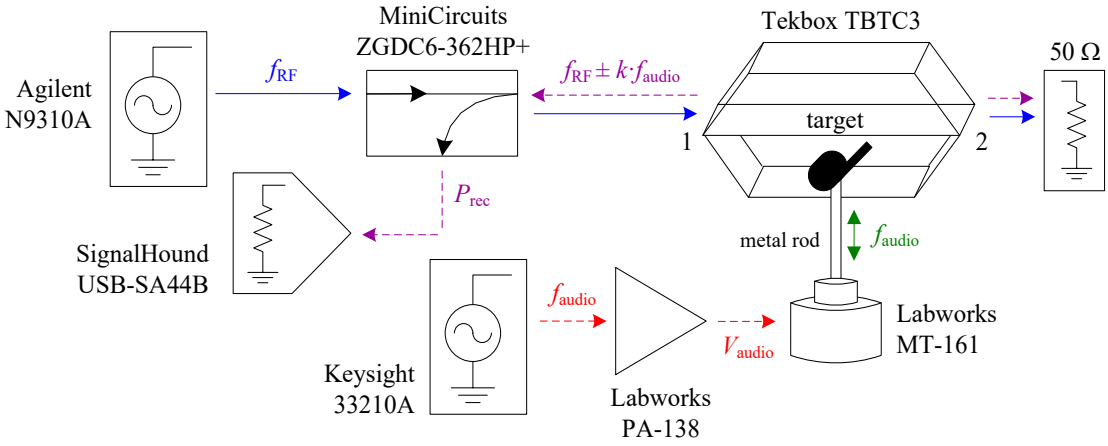

Fig. 3 Flowchart of acousto-EM experiment for studying responses of targets to excitation by acoustic-radar probes.

A rigid ("stinger") rod extends from the LabWorks MT-161 modal thruster (shaker) to the target. (To eliminate mechanical resonances in the modal-thruster system and lower the acousto-RF noise floor of the experiment, this 1-ft-long metal rod will be replaced by a 2-ft-long fiberglass rod for future experiments.) The target is attached to the rod using a pair of rare-earth magnets. The thruster is powered by the LabWorks PA-138 audio amplifier into which is fed an audio frequency signal at f_{audio} provided by the Keysight 33210A function generator. The gain of the PA-138 amp is adjusted to provide V_{audio} = 570 mV_{RMS} to the MT-161 thruster.

The thruster vibrates the rod, and the rod vibrates the target. The EM wave reflected by the target (while it is illuminated by f_{RF} and shaking at a frequency of f_{audio}) is sent back out Port 1 of the TEM cell. This backward-traveling reflection is sampled (at –6 dB) by the directional coupler. The sampled P_{rec} is sent from the coupled port of the ZGDC6 unit to the SignalHound USB-SA44B spectrum analyzer.

Pictures of the experiment (diagrammed in Fig. 3) are given in Figs. 4 and 5. A computer running Matlab controls the RF generator, audio generator, and spectrum analyzer. A script written to use the Matlab Instrument Control Toolbox automates the sweeps of f_{RF} and f_{audio} and captures power spectra (P_{rec}) across the frequency range $[f_{RF} - 5f_{audio}, f_{RF} + 5f_{audio}]$. This script is provided in the Appendix.

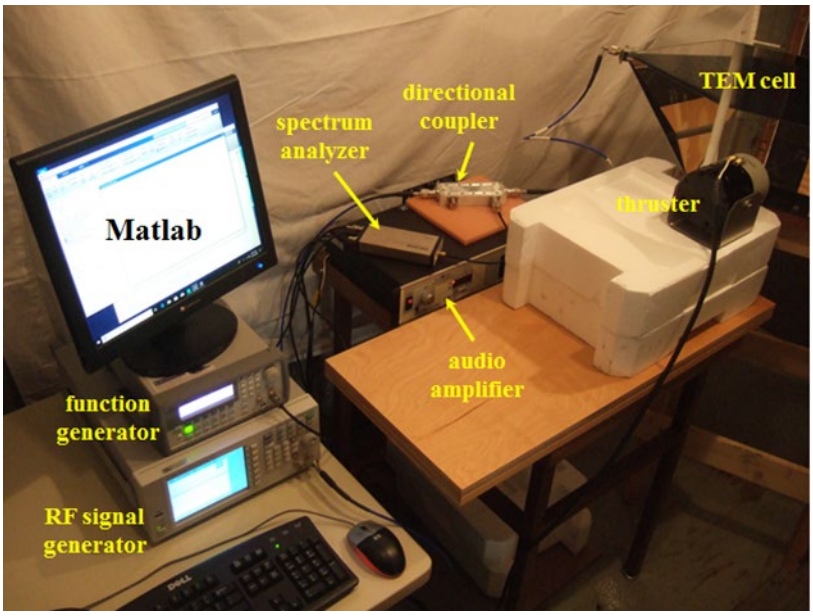

Fig. 4 Acousto-EM experiment: signal generation and capture system

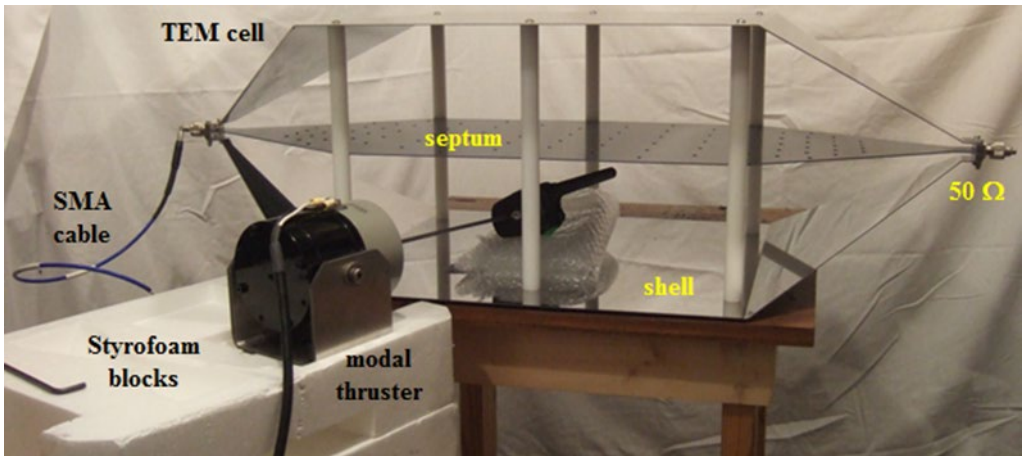

Fig. 5 Acousto-EM experiment: TEM cell and modal thruster

The TEM cell and modal thruster are mounted atop separate wooden tables to isolate vibrations from one unit to the other. The thruster itself sits atop a pair of Styrofoam blocks. The height from the lower part of the TEM shell to the septum that runs along the center of the cell is 15 cm. The effective width and depth of the target emplacement area (between the vertical white standoffs) is 50 × 34 cm. This particular TEM cell was manufactured to study RF responses up to 730 MHz.[9] The shorter, narrower TBTC2 and TBTC1 cells accommodate RF excitations up to approximately 3 GHz. The higher-frequency capability is traded off against reduced volume for target emplacement. The smaller volumes restrict not only the size of targets that may be probed, but also the set of target. Orientations that may

be studied. To study targets taller than a soda can and/or those with long vertical antennas (i.e., aligned parallel to the electric field of the incident radar wave), a wideband horn antenna should be substituted for the TEM cell.

3. Data

To study the acoustic-radar responses of electronics, three handheld radios were selected as targets (Fig. 6). Also, three clutter items were studied: machine screws and nuts, which represent metallic clutter containing many conductive junctions, and a soda can that represents slightly larger clutter that is metallic but contains few conductive junctions (Fig. 7).

Fig. 6 Handheld radio targets: Motorola MD200R, Midland LXT118, and Uniden GMR1636-2C

Fig. 7 Radar clutter items: (left) bag of 1/2-inch machine screws (×50) and bag of 3/8-inch nuts (×50), and (right) 12-oz soda can

A sample power spectrum recorded from the GMR1636 radio is shown in Fig. 8. While this data trace was recorded, the radio was illuminated by f_{RF} = 410 MHz and f_{audio} = 200 Hz. The resolution bandwidth of the USB-SA44B analyzer was set to 20 Hz. (This setting is adjusted to 1/10th of f_{audio} for each capture.) The true power received is actually 6 dB higher than that displayed in the figure because the directional coupler samples P_{rec} at 6 dB below the radar reflection. As expected for a target that contains many conductive and semi-conductive junctions, acousto-EM energy at $f_{RF} \pm n \cdot f_{audio}$ is evident for n = 1…4 (and likely n > 4, outside the data-capture range).

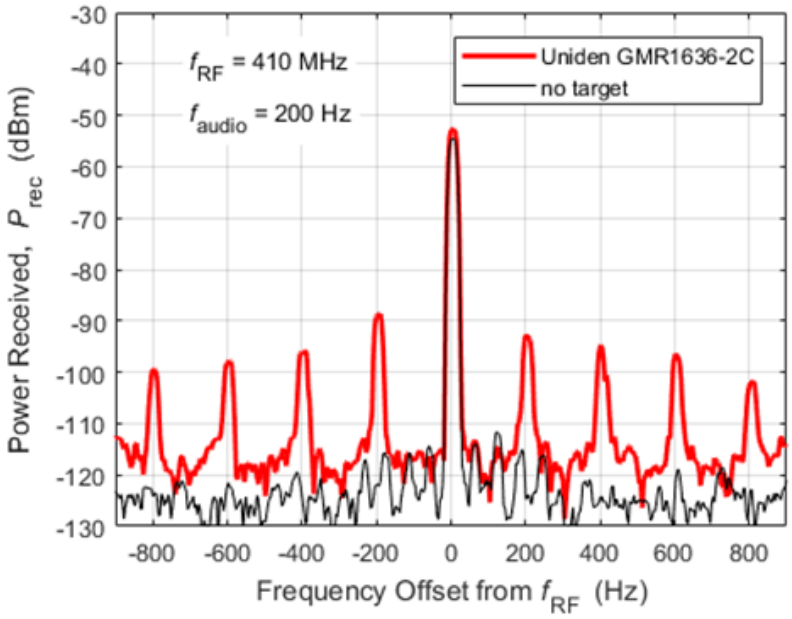

Fig. 8 Acoustic-radar response of the Uniden GMR1636-2C radio: single P_{rec} trace recorded for f_{RF} = 410 MHz and f_{audio} = 200 Hz

A processed set of power spectra, recorded from the Motorola MD200R radio, is shown in Fig. 9. The average power recorded for n = 1 ($f_{RF} \pm f_{audio}$) is plotted for a set value of f_{audio} = 200 Hz and a sweep of f_{RF} across the range [300 MHz, 800 MHz]. The response of this target is particularly strong at f_{RF} = 410 MHz, with a signal level above the no-target case (system noise floor) of ΔP_{rec} = 47 dB.

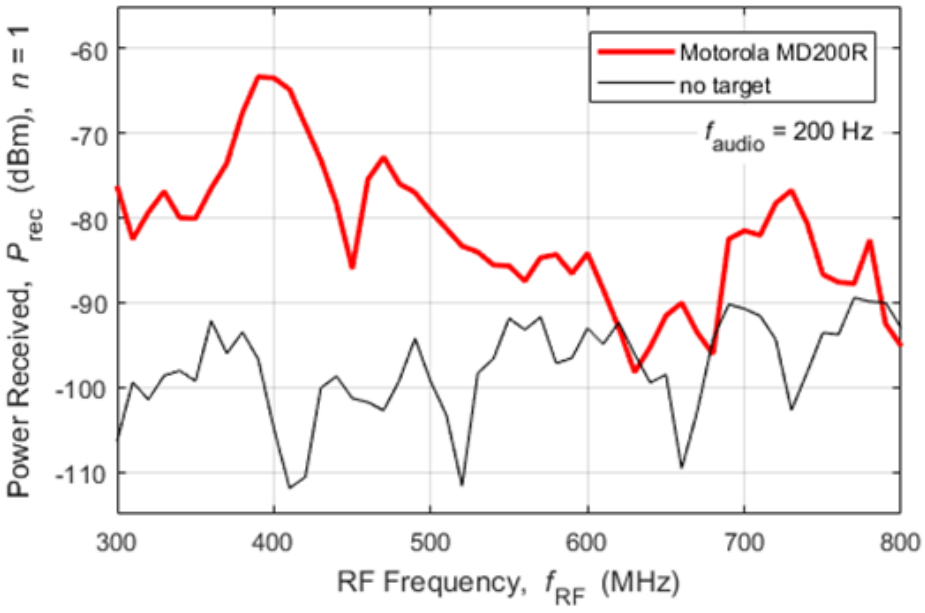

Fig. 9 Acoustic-radar response of the Motorola MD200R radio: P_{rec} at n = 1, recorded for f_{audio} = 200 Hz across f_{RF} = [300 MHz, 800 MHz]

Responses above the system noise, for all three radios and n = 1, across an RF sweep range of [300 MHz, 800 MHz] and an audio sweep range of [50 Hz, 800 Hz], are given in Fig. 10.

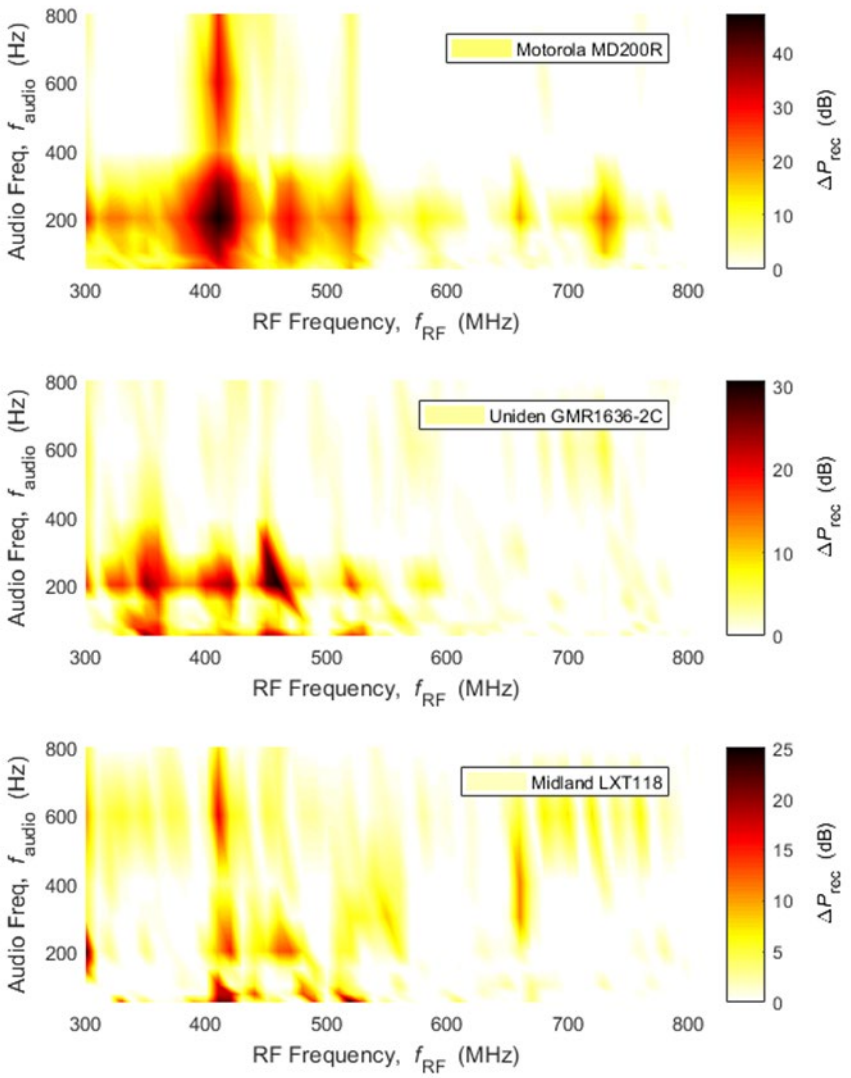

Fig. 10 Acoustic-radar response of handheld radios: ΔP_{rec} at n = 1, recorded across f_{RF} = [300 MHz, 800 MHz] and f_{audio} = [50 Hz, 800 Hz]

The MD200R radio is particularly responsive at f_{RF} = 410 MHz and most f_{audio} values, as well as at f_{audio} = 200 Hz and most f_{RF} values. The GMR1636 radio is consistently responsive at f_{audio} = 200 Hz and below f_{RF} = 490 MHz. The LXT188 radio is the least responsive of the three, but it is generally still detectable at f_{audio} = 50 Hz and below f_{RF} = 530 MHz.

A similar 2-D frequency sweep was performed on the radar-clutter items. Those results are shown in Fig. 11.

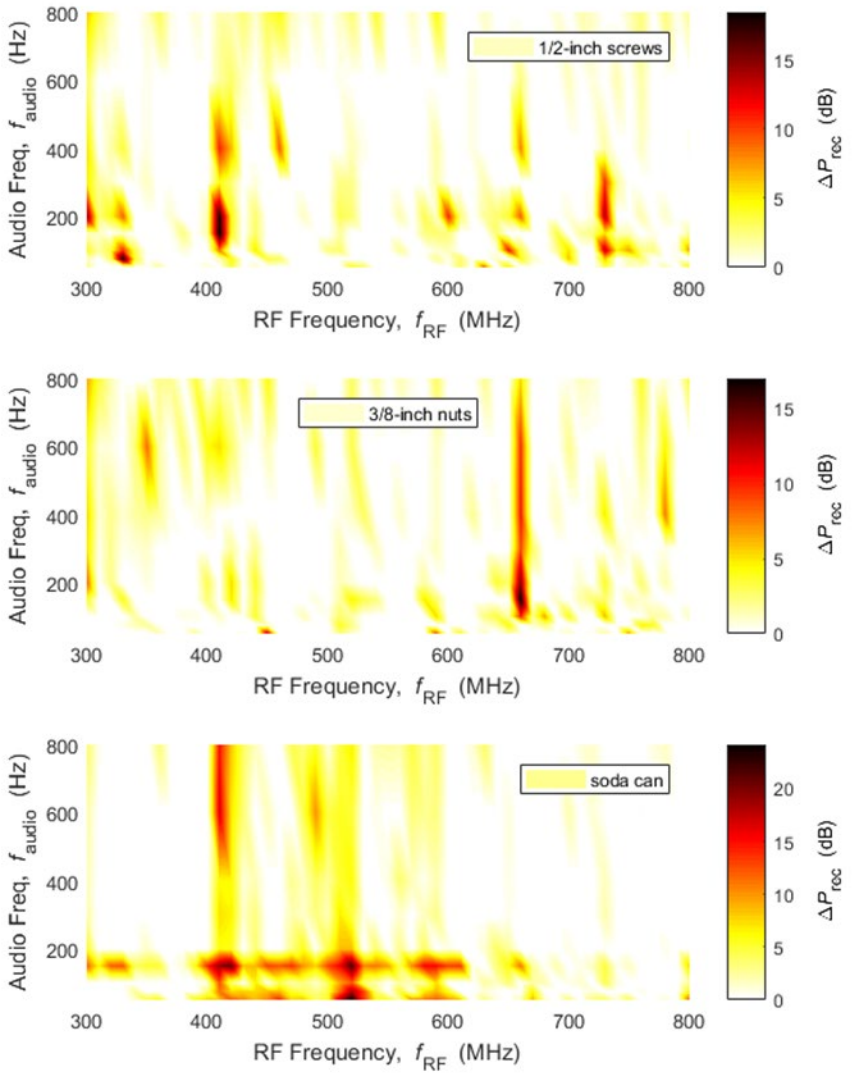

Fig. 11 Acoustic-radar response of radar-clutter items: ΔP_{rec} at n = 1, recorded across f_{RF} = [300 MHz, 800 MHz] and f_{audio} = [50 Hz, 800 Hz]

The 1/2-inch machine screws are barely detectable above the system noise except for a handful of RF and audio combinations such as f_{RF} = 410 MHz and f_{audio} = 200 Hz. The 3/8-inch nuts are consistently responsive at f_{RF} = 660 MHz. The 12-oz soda can is responsive mostly at f_{audio} = 150 Hz within the RF band f_{RF} = [400 MHz, 610 MHz].

A sample RF sweep, recorded from the soda can, is shown in Fig. 12. A sample single spectrum, recorded from the 3/8-inch nuts, is shown in Fig. 13.

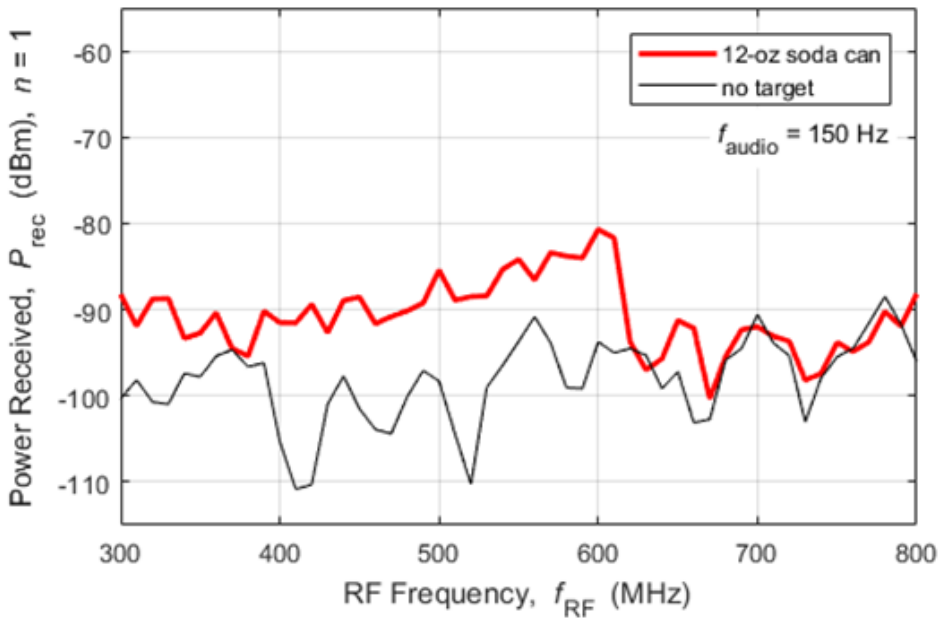

Fig. 12 Acoustic-radar response of the 12-oz soda can: P_{rec} at n = 1, recorded for f_{audio} = 150 Hz across f_{RF} = [300 MHz, 800 MHz]

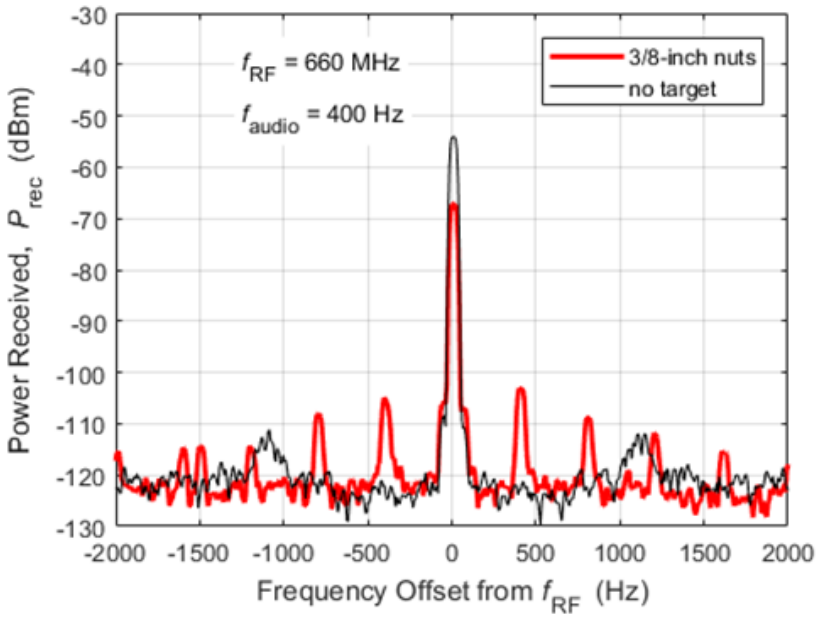

Fig. 13 Acoustic-radar response of the bag of 3/8-inch nuts: single P_{rec} trace recorded for f_{RF} = 660 MHz and f_{audio} = 400 Hz

4. Conclusions

Excitation of radar targets with acoustic and EM energy simultaneously was accomplished using a modal thruster that extends into a TEM cell. The modal thruster vibrates the target at the frequency f_{audio}, while the TEM cell illuminates the target with RF energy at the frequency f_{RF}. Acousto-EM interactions at the target impart audio modulation onto the RF carrier. Radar waves reflected from the target at multiples of f_{audio} above or below f_{RF} indicate detection of the target. During this study, responses were recorded from three handheld radios and three metallic radar-clutter items across the frequency ranges f_{RF} = [300 MHz, 800 MHz] and f_{audio} = [50 Hz, 800 Hz]. All six devices exhibited acousto-EM behavior, detectable above the system noise, for frequency combinations within this range.

This experiment will soon be extended to higher radio frequencies, a finer resolution of audio frequencies, and additional defense-related targets of interest.

5. References

1. Mazzaro GJ, Sherbondy AJ, Judy MR, Gallagher KA. Detection of metallic and electronic radar targets by acoustic modulation of electromagnetic waves. Aberdeen Proving Ground (MD): Army Research Laboratory (US); 2017 July. Report No.: ARL-TR-8076.

2. Buerkle A, Sarabandi K. Non-destructive evaluation of elastic targets using acousto-electromagnetic wave interaction and time reversal focusing. IEEE Transactions on Antennas Propagation. 2009;57(11):3628–3637.

3. Scott WR, Larson GD, Martin JS. Simultaneous use of elastic and electromagnetic waves for the detection of buried land mines. Proceedings of SPIE, Detection and Remediation Technologies for Mines and Mine-like Targets. 2000;4038:667–678.

4. Johnson SJ. Modulation of radio frequency signals by nonlinearly generated acoustic fields [doctoral dissertation]. [Raleigh (NC)]: North Carolina State University; 2014 Sept.

5. Origlio GF. The METRRA techniques. Ft Belvoir (VA): Army Mobility Equipment Research and Development Center (US); 1972.

6. Mazzaro GJ, Sherbondy AJ, Judy MR, Gallagher KA, Sherbondy KD. Detection of radio-frequency electronics by acoustic modulation of radar waves. Proceedings of Radar Sensor Technology XXII; 2018 May; Orlando, FL. SPIE Defense and Security. 2018;10633:1–13.

7. Wetherington JM, Steer MB. Standoff acoustic modulation of radio frequency signals in a log-periodic dipole array antenna. IEEE Antennas and Wireless Propagation Letters. 2012;11:885–888.

8. Mazzaro GJ. Hardware simulation of harmonic radar using a transverse electromagnetic cell. Proceedings of IEEE 2018 SoutheastCon; 2018 Apr 19–22; St Petersburg, FL.

9. Mayerhofer M. Open TEM cells for EMC pre-compliance testing product datasheet. Fairport (NY): Tekbox Digital Solutions; 2016 Apr.

Appendix. Matlab Code for Automated RF and Audio Frequency Sweeps

This Appendix appears in its original form without editorial change.

```
%%%%%%%%%%%%%%%%%%%%%%%%%%%%%%%%%%%%%%%%%%%%%%%%%%%%%%%%%%%%%%%%%%%%%%%
%%% set frequencies to sweep & power levels to output %%%
%%%%%%%%%%%%%%%%%%%%%%%%%%%%%%%%%%%%%%%%%%%%%%%%%%%%%%%%%%%%%%%%%%%%%%%

freq_RF = 300e6:10e6:800e6;                                % RF
frequencies
freq_audio = [50 75 100 150 200 300 400 600 800];          % audio
frequencies

pwr_RF = 0;                                                % RF power
(dBm)
pwr_audio = 0;                                             % audio
power (dBm)

ref_level = -10;

%%%%%%%%%%%%%%%%%%%%%%%%%%%%%%%%%%%%%%%%%%%%%%%%%%%%%%%%%%%%%%%%%%%%%%%

A = sqrt(10^(pwr_audio/10)*2*50*10^-3);                    % audio
amplitude (V)

%%%%%%%%%%%%%%%%%%%%%%%%%%%%%%%%%%%%%%%%%%%%%%%%%%%%%%%%%%%%%%%%%%%%%%%
%%% initialize Agilent N9310A RF signal generator %%%
%%%%%%%%%%%%%%%%%%%%%%%%%%%%%%%%%%%%%%%%%%%%%%%%%%%%%%%%%%%%%%%%%%%%%%%

awg = visa('agilent',
'USB0::0x0957::0x2018::0115000758::0::INSTR');
fopen(awg);
fprintf(awg, 'MOD:STATe OFF');
fprintf(awg, ['AMPLitude:CW ' num2str(pwr_RF) ' dBm']);
fprintf(awg, 'RFOutput:STATe ON');
fclose(awg);

%%%%%%%%%%%%%%%%%%%%%%%%%%%%%%%%%%%%%%%%%%%%%%%%%%%%%%%%%%%%%%%%%%%%%%%
%%% initialize Keysight 33210A function generator %%%
%%%%%%%%%%%%%%%%%%%%%%%%%%%%%%%%%%%%%%%%%%%%%%%%%%%%%%%%%%%%%%%%%%%%%%%

fng = gpib('ni', 0, 10);
set(fng,'OutputBufferSize',2^18);

%%%%%%%%%%%%%%%%%%%%%%%%%%%%%%%%%%%%%%%%%%%%%%%%%%%%%%%%%%%%%%%%%%%%%%%
%%% initialize SignalHound USB-SA44B spectrum analyzer %%%
%%%%%%%%%%%%%%%%%%%%%%%%%%%%%%%%%%%%%%%%%%%%%%%%%%%%%%%%%%%%%%%%%%%%%%%

specan = visa('agilent', 'TCPIP0::localhost::5025::SOCKET');
set(specan,'InputBufferSize',2^20);
fopen(specan);
fprintf(specan, ['SENSe:POWer:RF:RLEVel ' num2str(ref_level)] );
fprintf(specan, ['TRACe:TYPE AVERage']);
fprintf(specan, ['TRACe:AVERage:COUNt 10']);
fclose(specan);

%%%%%%%%%%%%%%%%%%%%%%%%%%%%%%%%%%%%%%%%%%%%%%%%%%%%%%%%%%%%%%%%%%%%%%%
%%% sweep RF and audio frequencies %%%
%%%%%%%%%%%%%%%%%%%%%%%%%%%%%%%%%%%%%%%%%%%%%%%%%%%%%%%%%%%%%%%%%%%%%%%
```

```
pwr_Nequals1 = zeros(length(freq_RF),length(freq_audio));

for counter_RF = 1:length(freq_RF)
    for counter_audio = 1:length(freq_audio)

        %%%%%%%%%%%%%%%%%%%%%%%%%%%%
        %%% set new RF frequency %%%
        %%%%%%%%%%%%%%%%%%%%%%%%%%%%

        fopen(awg);
        fprintf(awg, ['FREQuency:CW '
num2str(freq_RF(counter_RF)/10^6)...
                      ' MHz']);
        fclose(awg);

        pause(0.1);

        %%%%%%%%%%%%%%%%%%%%%%%%%%%%%%%%
        %%% set new audio frequency %%%
        %%%%%%%%%%%%%%%%%%%%%%%%%%%%%%%%

        fopen(fng);
        fprintf(fng, ['APPLy:SINusoid ' ...
                     num2str(freq_audio(counter_audio)) ','
num2str(A*2)]);
        fprintf(fng, ['OUTPut ON']);
        fclose(fng);

        pause(0.1);

        %%%%%%%%%%%%%%%%%%%%%%%%%%%%%%%%%%%%%%%%%%%%%%%%%%%%%%%%%%%%%%%%%%%%%%%
        %%% record power-vs-frequency from spectrum analyzer %%%
        %%%%%%%%%%%%%%%%%%%%%%%%%%%%%%%%%%%%%%%%%%%%%%%%%%%%%%%%%%%%%%%%%%%%%%%

        freq_center = freq_RF(counter_RF);
        freq_span = freq_audio(counter_audio) * 10;
        res_BW = freq_audio(counter_audio)/10;

        fopen(specan);
        fprintf(specan, ['TRACe:CLEar']);
        fprintf(specan, ['FREQuency:CENTer '
num2str(freq_center)] );
        fprintf(specan, ['FREQuency:SPAN ' num2str(freq_span)] );
        fprintf(specan, ['SENSe:BANDwidth:RESolution '
num2str(res_BW)] );

        pause(10);
        fprintf(specan, ['TRACe:DATA? TRACE1']);
        pause(0.25);

        data = fscanf(specan);
        fclose(specan);


%%%%%%%%%%%%%%%%%%%%%%%%%%%%%%%%%%%%%%%%%%%%%%%%%%%%%%%%%%%%%%%%%%%%%%%
```

```
        %%% extract power in n=1 sideband from P-vs-freq trace
%%%

%%%%%%%%%%%%%%%%%%%%%%%%%%%%%%%%%%%%%%%%%%%%%%%%%%%%%%%%%%%%%%%%

        freq_start = freq_center - freq_span/2;
        freq_stop = freq_center + freq_span/2;

        data_raw = strsplit(data,',');
        pwr_data = str2num(char(data_raw))';
        freq_delta = freq_span/(length(pwr_data)-1);
        freq_data = [freq_start:freq_delta:freq_stop];

        freq_minus1_L = freq_RF(counter_RF)-
1.5*freq_audio(counter_audio);
        freq_minus1_R = freq_RF(counter_RF)-
0.5*freq_audio(counter_audio);
        [y,index_minus1_L] = min( abs(freq_data - freq_minus1_L)
);
        [y,index_minus1_R] = min( abs(freq_data - freq_minus1_R)
);
        pwr_minus1 = max( pwr_data(index_minus1_L:index_minus1_R)
);

        freq_plus1_L =
freq_RF(counter_RF)+0.5*freq_audio(counter_audio);
        freq_plus1_R =
freq_RF(counter_RF)+1.5*freq_audio(counter_audio);
        [y,index_plus1_L] = min( abs(freq_data - freq_plus1_L) );
        [y,index_plus1_R] = min( abs(freq_data - freq_plus1_R) );
        pwr_plus1 = max( pwr_data(index_plus1_L:index_plus1_R) );

        pwr_Nequals1(counter_RF,counter_audio) = log10(
(10.^pwr_minus1 ...
                                                        +
10.^pwr_plus1)/2 );

        pause(0.1)

        %%%%%%%%%%%%%%%%%%%%%%%%%%%%%%%%%%%%%%%%%%%%%
        %%% save each power-vs-frequency trace %%%
        %%%%%%%%%%%%%%%%%%%%%%%%%%%%%%%%%%%%%%%%%%%%%

        save(['acoustoRF_trace_' ...
              num2str(freq_RF(counter_RF)/10^6) 'MHz_'...
              num2str(freq_audio(counter_audio)) 'Hz.mat'], ...
              'freq_data','pwr_data');
    end
end

%%%%%%%%%%%%%%%%%%%%%%%%%%%%%%%%%%%%%%%%%%%%%%%%%%%%%%%%%%%%%%%%
%%% turn off RF and audio signal sources %%%
%%%%%%%%%%%%%%%%%%%%%%%%%%%%%%%%%%%%%%%%%%%%%%%%%%%%%%%%%%%%%%%%

fopen(awg);
fprintf(awg, 'RFOutput:STATe OFF');
```

```
fclose(awg);

fopen(fng);
fprintf(fng, ['OUTPut OFF']);
fclose(fng);

%%%%%%%%%%%%%%%%%%%%%%%%%%%%%%%%%%%%%%%%%%%%%%%%%%%%%%%%%%%%%%%%%%%%%%%
%%% generate a 3D plot of power-vs-frequency results %%%
%%%%%%%%%%%%%%%%%%%%%%%%%%%%%%%%%%%%%%%%%%%%%%%%%%%%%%%%%%%%%%%%%%%%%%%

[f_RF,f_audio] = meshgrid(freq_RF,freq_audio);

f_RF = f_RF';   f_audio = f_audio';

figure
pcolor(f_RF/10^6,f_audio,pwr_Nequals1);
view(0,90);
colormap copper; shading interp; colorbar;
xlabel('RF Frequency  (MHz)')
ylabel('Audio Frequency  (Hz)')

save(['acoustoRF_sweep_' num2str(freq_RF(1)/10^6) 'to' ...
      num2str(freq_RF(length(freq_RF))/10^6) 'MHz_' ...
      num2str(freq_audio(1)) 'to' ...
      num2str(freq_audio(length(freq_audio))) 'Hz.mat'], ...
      'f_RF','f_audio','pwr_Nequals1');
```

List of Symbols, Abbreviations, and Acronyms

2-D	2-dimensional
CW	continuous wave
EM	electromagnetic
f_{audio}	single acoustic frequency
f_{RF}	single radio frequency
RF	radio frequency
Rx	receiver
TEM	transverse electromagnetic
Tx	transmitter
Tx_{RF}	electromagnetic transmission
UHF	ultra-high frequency
USB	Universal Series Bus

1 (PDF)	DEFENSE TECHNICAL INFORMATION CTR DTIC OCA
2 (PDF)	DIR ARL IMAL HRA RECORDS MGMT RDRL DCL TECH LIB
1 (PDF)	GOVT PRINTG OFC A MALHOTRA
4 (PDF)	ARL RDRL SER U A SULLIVAN G MAZZARO K GALLAGHER K SHERBONDY